Variance Swap with Mean Reversion, Multifactor Stochastic Volatility and Jumps

Pun, Chi Seng; Chung, Shing Fung; Wong, Hoi Ying

2015

Pun, C. S., Chung, S. F., & Wong, H. Y. (2015). Variance swap with mean reversion, multifactor stochastic volatility and jumps. European Journal of Operational Research, 245(2), 571-580.

https://hdl.handle.net/10356/81385

https://doi.org/10.1016/j.ejor.2015.03.026

Variance Swap with Mean Reversion, Multifactor Stochastic Volatility and Jumps

Chi Seng Pun, Shing Fung Chung and Hoi Ying Wong [1]
Department of Statistics
The Chinese University of Hong Kong, Shatin, Hong Kong

Abstract

This paper examines variance swap pricing using a model that integrates three major features of financial assets, namely the mean reversion in asset price, multi-factor stochastic volatility (SV) and simultaneous jumps in prices and volatility factors. Closed-form solutions are derived for vanilla variance swaps and gamma swaps while the solutions for corridor variance swaps and conditional variance swaps are expressed in a one-dimensional Fourier integral. The numerical tests confirm that the derived solution is accurate and efficient. Furthermore, empirical studies have shown that multi-factor SV models better capture the implied volatility surface from option data. The empirical results of this paper also show that the additional volatility factor contributes significantly to the price of variance swaps. Hence, the results favor multi-factor SV models for pricing variance swaps consistent with the implied volatility surface.

Keywords: Pricing, Variance Swap, Multi-factor Stochastic Volatility, Mean Reversion, Jump Diffusion

[1]Correspondence author; fax: (852) 2603-5188; e-mail: hywong@cuhk.edu.hk.

1. Introduction

The management of volatility risk has gained increased attention in financial markets since the onset of the recent global financial crisis. Variance swap is a typical financial tool for managing this risk. Numerous researches have been done on variance swaps (Carr and Madan, 1998; Demeterfi et al., 1999). However, none of them consider the discrete monitoring principle or the use of stochastic volatility model. Until recently, Zhu and Lian (2011) solve the discretely sampled variance swap pricing formula under the Heston's stochastic volatility (SV) model using a partial differential equation (PDE) approach. Zheng and Kwok (2012) consider the stochastic volatility simultaneous jump (SVSJ) model in the valuation of various types of variance swap contracts using a probabilistic approach. They also include saddle-point approximation in Zheng and Kwok (2013a) and Fourier transform algorithms in Zheng and Kwok (2013b), respectively, in variance swap pricing under Lévy processes.

In this paper, we generalize these recent advances in variance swap pricing to a wider class of models that incorporates the following well-known features of financial asset dynamics: mean reversion in asset price, multi-factor SV and simultaneous jumps in price and volatility factors. Therefore, the model considered embraces the Heston SV and SVSJ models as its special cases. Mean reversion is a well-known feature in commodity markets. A list of empirical studies supporting the existence of mean reversion can be found in Fusai et al. (2008). Wong and Lo (2009) propose an option pricing model with mean reversion and the Heston SV to capture information contained in the term structure of futures prices. The Wong and Lo model is also found to be a special case of our model.

Another well-known empirical finding is that the implied volatility surface

solved by matching market option prices and the Black-Scholes formula shows a smiling pattern. Numerous models have been proposed to capture this pattern, including the SV models. Empirical evidence, however, shows that the level of implied volatility is independent of the slope of the volatility smile. Although a one-factor SV model can generate a steep smile or a flat smile for a given volatility, it fails to generate both patterns for a given parameterization. Using the Black-Scholes implied volatility for S&P 500 options over 15 years, the empirical study by Christoffersen et al. (2009) shows that a two-factor SV model is sufficient to model the stock return volatility based on a principal component analysis. The empirical study by Li and Zhang (2010) confirms the existence of the second volatility factor using a nonparametric test. Therefore, we consider a two-factor SV model in this paper.

Apart from mean reversion and multifactor SV, jumps in the return process and volatility factors have also received a great deal of research attention. Jacod and Todorov (2010) discover that the prices of most of the constituent stocks in the S&P 500 index jump together with their volatilities. Duffie et al. (2000) compare an SV model without jumps, an SV model with jump in price and an SVSJ model and show that the SVSJ model is able to produce an implied volatility smile closest to the one observed in the market. Wong and Zhao (2010) apply a model with mean reversion and two SV factors to currency option pricing. However, they do not incorporate jumps nor investigate the implications of their model for variance swap pricing.

In this paper, we value various types of discretely monitored variance swaps under the proposed model. We follow Zheng and Kwok (2012) in using the square of the geometric return of the underlying asset to represent the realized variance in

the variance swaps. The solution for the fair strike price in the variance swap contract, or the variance swap price, relies on the analytic joint characteristic function of the log asset prices at two different time points. We obtain this characteristic function by first deriving the joint characteristic function of the log asset price and its volatility at a particular time point. Then, we transform the payoff function of the variance swap into an exponential function. This enables the variance swap price to be deduced from the characteristic function.

The remainder of this paper is organized as follows. The proposed model is presented in Section 2, where we also derive the joint characteristic function of the log asset price and the volatility. The analytical formulas for various types of variance swap contracts are obtained in Section 3. Empirical and numerical experiments are conducted in Section 4. Specifically, the empirical experiments illustrate the effect of the second volatility factor on variance swap prices. Section 5 concludes the paper.

2. The Model

Under the risk-neutral measure, we postulate that the underlying asset S_t and its two volatility factors V_{1t} and V_{2t} jointly evolve as follows. Let $S_t = \exp(X_t)$.

$$\begin{aligned} dX_t &= [\theta(t) - mX_t - \tfrac{V_{1t}+V_{2t}}{2}]dt + \sqrt{V_{1t}}dW_t^1 + \sqrt{V_{2t}}dW_t^3 + J_t^X dN_t^1, \\ dV_{1t} &= [a_1(t) - b_1 V_{1t}]dt + \sigma_1\sqrt{V_{1t}}[\rho_1 dW_t^1 + \sqrt{1-\rho_1^2}dW_t^2] + J_t^{V_1} dN_t^1, \\ dV_{2t} &= [a_2(t) - b_2 V_{2t}]dt + \sigma_2\sqrt{V_{2t}}[\rho_2 dW_t^3 + \sqrt{1-\rho_2^2}dW_t^4] + J_t^{V_2} dN_t^2, \end{aligned} \tag{1}$$

where W_t^1, W_t^2, W_t^3 and W_t^4 are independent standard Wiener processes; N_t^1 and N_t^2 are independent Poisson processes with constant intensities λ_1 and λ_2, respectively; and J^{V_2}, J^{V_1} and J^X are independent random variables that repre-

sent random jump sizes and which are independent of the Wiener processes and Poisson processes.

This model (1) embraces most of the important derivatives pricing models in the literature. The simultaneous jumps on asset return and its volatility considered by Zheng and Kwok (2012) are reflected by the Poisson process N_t^1, while N_t^2 models jumps in the volatility process independent of the asset return. The constant m is the mean-reversion speed of the log asset, the deterministic function $\theta(t)$ is related to the equilibrium mean level of the log asset at time t and J^X denotes the random jump size of the log asset. Similarly, the constant b_i is the mean-reversion speed of the ith volatility factor, the deterministic function $a_i(t)$ is related to the equilibrium mean level of the ith volatility factor at time t, the constant σ_i is the volatility coefficient of the ith volatility factor process and J^{V_i} denotes the random jump size of the ith volatility factor for $i = 1, 2$. Notice that it is not necessary to know the explicit form of $\theta(t)$ since we will show in later part that this term can be calibrated with futures as a whole. If there is no jump, the model is reduced to the mean reversion model with two-factor SV in Wong and Zhao (2010). If the mean-reversion speed m is further set to zero, it becomes the two-factor SV model proposed by Christoffersen et al. (2009).

2.1. The Characteristic Function

The payoff of variance swaps depends on the underlying asset prices realized at time points $0 < t_1 < \cdots < t_n$. Thus, the valuation needs the joint distribution of asset prices at these time points. We thus derive the multivariate characteristic function of log-spot prices, $\ln S_{t_1}, \cdots, \ln S_{t_n}$, under the proposed model and then apply the results to the variance swap pricing in the next section.

This section is organized as follows. We begin with a mean reversion model

with a one-factor SV and extend it to incorporate the second SV factor. As shown in the later analysis, the process with two SV factors can be written as the sum of two independent processes with one SV factor. As the building block for the later analysis, the following lemma presents the joint characteristic function of the log-asset value and its variance under the mean reversion model with a one-factor SV process and simultaneous jumps. Afterward we derive the joint characteristic function of the log-asset values under the model (1).

Lemma 2.1. Consider the mean reversion model with SV and simultaneous jumps:

$$\begin{aligned} dX_t &= [\theta(t) - mX_t - \tfrac{V_t}{2}]dt + \sqrt{V_t}dW_t^1 + J_t^X dN_t, \\ dV_t &= [a(t) - bV_t]dt + \sigma\sqrt{V_t}[\rho dW_t^1 + \sqrt{1-\rho^2}dW_t^2] + J_t^V dN_t, \end{aligned} \tag{2}$$

where W_t^1 and W_t^2 are independent standard Wiener processes; N_t is a Poisson process with constant intensity λ independent of the two Wiener processes; and J_t^X and J_t^V are random jump sizes of the log asset price and volatility, respectively. J_t^X and J_t^V are independent of the two Wiener processes and the Poisson process. Then, the joint characteristic function of X_t and V_t is given by

$$f(x,v,t;\phi,\varphi) = \mathbb{E}\left[\exp(i\phi X_T + i\varphi V_T)|X_t = x, V_t = v\right] \tag{3}$$

$$= \exp[A(T-t;\phi)x + B(T-t;\phi,\varphi)v + C(T-t;\phi,\varphi)], \tag{4}$$

where $T \geq t$ and $i = \sqrt{-1}$,

$$\begin{aligned} A(\tau;\phi) &= i\phi e^{-m\tau}, \\ B(\tau;\phi,\varphi) &= U(e^{-m\tau}) + \frac{e^{-b\tau}V(e^{-m\tau})}{\frac{1}{i\varphi - U(1)} + \frac{\sigma^2}{2m}\int_1^{e^{-m\tau}} y^{\frac{b}{m}-1}V(y)dy}, \\ C(\tau;\phi,\varphi) &= \int_{T-\tau}^{T} [\theta(s)A(T-s;\phi) + a(s)B(T-s;\phi,\varphi) \\ &\qquad + \lambda\mathbb{E}[\exp(A(T-s;\phi)J^X + B(T-s;\phi,\varphi)J^V) - 1]]ds, \end{aligned}$$

$$
\begin{aligned}
U(y;\phi) &= \frac{2my}{\sigma^2}\frac{(\sqrt{1-\rho^2}-\rho i)\frac{\sigma\phi}{2m}\Phi(a^*,b^*,\frac{y}{\omega(\phi)})+\frac{a^*}{b^*\omega(\phi)}\Phi(a^*+1,b^*+1,\frac{y}{\omega(\phi)})}{\Phi(a^*,b^*,\frac{y}{\omega(\phi)})},\\
V(y;\phi) &= \frac{\Phi^2(a^*,b^*,\frac{1}{\omega(\phi)})}{\Phi^2(a^*,b^*,\frac{y}{\omega(\phi)})}e^{\frac{\sigma\phi}{m}(1-y)\sqrt{1-\rho^2}},\\
a^* &= \frac{(\sqrt{\rho^2-1}+\rho)\frac{b^*}{2}+\frac{\sigma}{4m}}{\sqrt{\rho^2-1}},\ \ b^*=1-\frac{b}{m},\ \ \omega(\phi)=\frac{-m}{\sigma\phi\sqrt{1-\rho^2}},
\end{aligned}
$$

and $\Phi(\bullet,\bullet,\bullet)$ is the degenerated hypergeometric function.

Proof. The Feynman-Kac formula states that $f(x,v,t)$ is governed by the following partial integro-differential equation (PIDE):

$$
\begin{cases}
-\frac{\partial f}{\partial t} &= [\theta(t)-mx-\frac{v}{2}]\frac{\partial f}{\partial x}+[a(t)-bv]\frac{\partial f}{\partial v}+\frac{v}{2}\frac{\partial^2 f}{\partial x^2}+\frac{\sigma^2 v}{2}\frac{\partial^2 f}{\partial v^2}+\rho\sigma v\frac{\partial^2 f}{\partial x\partial v}\\
&\quad +\lambda\mathbb{E}[f(x+J^X,v+J^V,t)-f(x,v,t)],\\
f(x,v,T) &= \exp(i\phi x+i\varphi v).
\end{cases}
$$

From the affine structure of our model, we postulate $f(x,v,t)$ admitting the form (4). Substituting (4) into the above PIDE gives the following system of ordinary differential equations for A, B and C:

$$
\begin{aligned}
\frac{\partial A}{\partial \tau} &= -mA(\tau),\\
\frac{\partial B}{\partial \tau} &= \frac{\sigma^2}{2}B^2(\tau)-[b-\rho\sigma A(\tau)]B(\tau)-\frac{1}{2}A(\tau)[1-A(\tau)], \qquad (5)\\
\frac{\partial C}{\partial \tau} &= \theta(t)A(\tau)+a(t)B(\tau)+\lambda\mathbb{E}[\exp(A(\tau)J^X+B(\tau)J^V)-1], \qquad (6)
\end{aligned}
$$

with the initial conditions $A(0)=i\phi$, $B(0)=i\varphi$ and $C(0)=0$, where $\tau=T-t$ and (5) is known as the Riccati equation. It is trivial to solve for $A(\tau)$ and the explicit formula is displayed in this lemma. Substituting $A(\tau)$ into (5) gives:

$$
\begin{cases}
\frac{\partial B}{\partial \tau} &= \frac{\sigma^2}{2}B^2(\tau)-[b-\rho\sigma i\phi e^{-m\tau}]B(\tau)-\frac{1}{2}(i\phi e^{-m\tau}+\phi^2 e^{-2m\tau}),\\
B(0) &= i\varphi.
\end{cases}
$$

Following the results of Wong and Lo [10], we can write the analytical formula of $B(\tau)$ where the initial condition of $B(\tau)$ is $i\varphi$ instead of 0. Having obtained $A(\tau)$ and $B(\tau)$, $C(\tau)$ is then obtained by integrating both sides of (6). $\square$

An explicit formula of $C(\tau)$ in Lemma 2.1 can be obtained once the distributions of J^V and J^X are specified. Observe that if J^V and J^X are independent of each other, the last expectation in the above expression can be calculated directly by using the marginal characteristic functions of J^V and J^X, respectively. However, to allow for a more flexible modeling, we consider a more complicated structure for J^V and J^X. Specifically, we employ the dependent structure in Zheng and Kwok (2012) that $J^V \sim \exp(\eta),\ J^X|J^V \sim \mathcal{N}(\nu + \rho_J J^V, \delta^2)$. The expectation in $C(\tau)$ can be computed as follows:

$$\begin{aligned}
&\mathbb{E}[\exp(A(\tau;\phi)J^X + B(\tau;\phi,\varphi)J^V) - 1] \\
=&\exp[A(\tau;\phi)\nu + \frac{1}{2}A^2(\tau;\phi)\delta^2](1 - [\rho_J A(\tau;\phi) + B(\tau;\phi,\varphi)]\eta)^{-1} - 1.
\end{aligned}$$

In particular for $J^X \equiv 0$, the expectation is equal to $(1 - B(\tau;\phi,\varphi)\eta)^{-1} - 1$. As the result in Lemma 2.1 is frequently used in the remaining text with different parameters, we introduce the following notation.

Definition 2.1. The one-factor SV model considered in Lemma 2.1 is denoted as $M(\Theta; J^X, J^V)$, where $\Theta = \{\theta(t), m, a(t), b, \sigma, \rho, \lambda\}$ is the parameter set characterizing the model except for the jump sizes.

The joint characteristic function of the log asset prices $\mathbf{X} = (X_{t_1}, \cdots, X_{t_n})$ is defined as

$$F_{\mathbf{X}}(x_0, v_{10}, v_{20}; u_1, \ldots, u_n) = \mathbb{E}\left[\exp\left(iu_1 X_{t_1} + \cdots + iu_n X_{t_n}\right) \mid X_0 = x_0, V_{10} = v_{10}, V_{20} = v_{20}\right], \tag{7}$$

where $u_1, \cdots, u_n$ are real numbers. The following theorem holds.

Theorem 2.1. Under model (1), the multivariate characteristic function of $\mathbf{X}$ defined in (7) is given by

$$\begin{aligned} & F_{\mathbf{X}}(x_0, v_{10}, v_{20}; u_1, u_2, \cdots, u_n) \\ = & \exp\left[\sum_{k=1}^{n} C_1(t_k - t_{k-1}; \phi_k, \varphi_{1,k}) + B_1(t_1; \phi_1, \varphi_{1,1}) v_{10} + i\phi_1 e^{-mt_1} x_0\right] \\ & \cdot \exp\left[\sum_{k=1}^{n} C_2(t_k - t_{k-1}; \phi_k, \varphi_{2,k}) + B_2(t_1; \phi_1, \varphi_{2,1}) v_{20}\right], \end{aligned}$$

where

$$\begin{aligned} \phi_k &= u_k + \phi_{k+1} e^{-m(t_{k+1}-t_k)},\ k = 1, \cdots, n-1;\ \phi_n = u_n, \\ \varphi_{j,k} &= -iB_j(t_{k+1} - t_k; \phi_{k+1}, \varphi_{j,k+1}),\ k = 1, \cdots, n-1;\ \varphi_{j,n} = 0, \text{ for } j = 1, 2, \\ \Theta_1 &= \{\theta(t), m, a_1(t), b_1, \sigma_1, \rho_1, \lambda_1\}, \\ \Theta_2 &= \{0, m, a_2(t), b_2, \sigma_2, \rho_2, \lambda_2\}, \end{aligned}$$

in which B_1, B_2 are the function B in Lemma 2.1 under the model $M(\Theta_1; J^X, J^{V_1})$ and $M(\Theta_2; 0, J^{V_2})$, respectively. Similarly, C_1, C_2 are the function C in Lemma 2.1 under the model $M(\Theta_1; J^X, J^{V_1})$ and $M(\Theta_2; 0, J^{V_2})$, respectively.

Proof. We only prove the case of $n = 2$. The case with an arbitrary n can be shown by the same principle or by induction. Given the initial values x_0, v_{10} and v_{20}, we decompose $\{X_t\}$ into the sum of two random processes $\{Y_t\}$ and $\{Z_t\}$, i.e. $X_t = Y_t + Z_t$, such that

$$\begin{cases} dY_t &= [\theta(t) - mY_t - \frac{V_{1t}}{2}]dt + \sqrt{V_{1t}} dW_t^1 + J_t^X dN_t^1 \quad , \ Y_0 = x_0, \\ dV_{1t} &= [a_1(t) - b_1 V_{1t}]dt + \sigma_1 \sqrt{V_{1t}}[\rho_1 dW_t^1 + \sqrt{1-\rho_1^2} dW_t^2] + J_t^{V_1} dN_t^1 \quad , \ V_{10} = v_{10}, \end{cases} \tag{8}$$

$$\begin{cases} dZ_t &= [-mZ_t - \frac{V_{2t}}{2}]dt + \sqrt{V_{2t}} dW_t^3 \quad , \ Z_0 = 0, \\ dV_{2t} &= [a_2(t) - b_2 V_{2t}]dt + \sigma_2 \sqrt{V_{2t}}[\rho_2 dW_t^3 + \sqrt{1-\rho_2^2} dW_t^4] + J_t^{V_2} dN_t^2 \quad , \ V_{20} = v_{20}. \end{cases} \tag{9}$$

From model (1), it is clear that $\{Y_t\}$ and $\{Z_t\}$ are independent processes. Then the bivariate characteristic function is given by

$$F_{X_{t_1},X_{t_2}}(u_1,u_2) \;=\; \mathbb{E}[\exp(iu_1X_{t_1}+iu_2X_{t_2})] = E_1\cdot E_2,$$

where $E_1=\mathbb{E}[\exp(iu_1Y_{t_1}+iu_2Y_{t_2})]$ and $E_2=\mathbb{E}[\exp(iu_1Z_{t_1}+iu_2Z_{t_2})]$. Notice that $\{Y_t\}$ and $\{Z_t\}$ follow models $M(\Theta_1;J^X,J^{V_1})$ and $M(\Theta_2;0,J^{V_2})$, respectively. By Lemma 2.1,

$$E_1 \;=\; \exp\left[C_1(t_1;\phi_1,\varphi_{1,1})+C_1(t_2-t_1;\phi_2,\varphi_{1,2})+i\phi_1e^{-mt_1}x_0+B_1(t_1;\phi_1,\varphi_{1,1})v_{10}\right],$$

and

$$E_2=\exp\left[C_2(t_1;\phi_1,\varphi_{2,1})+C_2(t_2-t_1;\phi_2,\varphi_{2,2})+B_2(t_1;\phi_1,\varphi_{2,1})v_{20}\right].$$

This shows the bivariate case while the multivariate case follows by induction. □

As a concrete example, consider the exponential jump sizes for the volatility factors, $J^{V_1}\sim\exp(\eta_1),\ J^{V_2}\sim\exp(\eta_2)$, and the normal jump size for the log asset return conditional on J^{V_1} and independent of J^{V_2}: $J^X|J^{V_1}\sim\mathcal{N}(\nu+\rho_JJ^{V_1},\delta^2)$. This consideration is consistent with Zheng and Kwok (2012). Therefore, the joint characteristic function of log-asset prices is obtained in an explicit closed-form solution, which is useful in examining distributional properties and rendering an efficient pricing scheme for financial derivatives. As this paper focuses on variance swap contracts, the explicit pricing formulas are provided in the next section[2]. In practice, the characteristic function is often expressed in terms of

[2]Even a general model is provided in this paper, we use a submodel in the empirical studies as there is no available asset embraced all the features. The improvement with respect to some characteristic is still unknown and to be explored as an interesting future topic.

observed market forward (futures) prices. This is known as the super-calibration of the model by enforcing it to be consistent with the market prices of futures contracts.

Corollary 2.1. Under the model (1), a forward price of the underlying asset with maturity T is given by

$$\begin{aligned} G(T) &= \mathbb{E}\left[e^{X_T} \mid X_0 = x_0, V_{10} = v_{10}, V_{20} = v_{20}\right] \\ &= \exp[e^{-mT}x_0 + B_1(T; -i, 0)v_{10} + B_2(T; -i, 0)v_{20} \\ &\quad + C_1(T; -i, 0) + C_2(T; -i, 0)] \end{aligned}$$

where the functions involved are defined in Theorem 2.1.

Proof. The proof follows by noting $G(T) = F(x_0, v_{10}, v_{20}; -i)$ and applying Theorem 2.1. □

To express the characteristic function in terms of observed market forward (futures) prices, we link the common terms in Corollary 2.1 and Theorem 2.1.

$$\begin{aligned} \int_0^T \theta(s)e^{-m(T-s)}ds &= \ln[G(T)] - B_1(T; -i, 0)v_{10} - B_2(T; -i, 0)v_{20} \\ &\quad - e^{-mT}x_0 - \tilde{C}_1(T; -i, 0) - C_2(T; -i, 0), \end{aligned}$$

where

$$\begin{aligned} \tilde{C}_1(\tau; \phi, \varphi) &= \int_{T-\tau}^T [a_1(s)B_1(T - s; \phi, \varphi) + \lambda_1\mathbb{E}[\exp(A_1(T - s; \phi)J^X \\ &\quad + B_1(T - s; \phi, \varphi)J^{V_1}) - 1]]ds. \end{aligned} \tag{10}$$

This enables the characteristic function to be expressed super-calibrated to (or in terms of) futures prices in the market, by noting that

$$\int_{t_{k-1}}^{t_k} \theta(s)e^{-m(t_k-s)}ds = \int_0^{t_k} \theta(s)e^{-m(t_k-s)}ds - e^{-m(t_k-t_{k-1})} \int_0^{t_{k-1}} \theta(s)e^{-m(t_{k-1}-s)}ds.$$

The following corollary is straightforwardly obtained by substitution of this equation, such that no θ appears in the expression of the joint characteristic function.

Corollary 2.2. Under the model (1), the multivariate characteristic function of $\mathbf{X}$ super-calibrated to the term structure of future prices is given by

$$\begin{aligned}
&F_{\mathbf{X}}(u_1, u_2, \cdots, u_n) \\
=&\prod_{k=1}^{n} \left[\frac{G(t_k)}{G(t_{k-1})^{e^{-m(t_k - t_{k-1})}}} \right]^{i\phi_k} \exp\left[\sum_{k=1}^{n} \tilde{C}_1(t_k - t_{k-1}; \phi_k, \varphi_{1,k}) + B_1(t_1; \phi_1, \varphi_{1,1}) v_{10} \right] \\
&\cdot \exp\left[\sum_{k=1}^{n} C_2(t_k - t_{k-1}; \phi_k, \varphi_{2,k}) + B_2(t_1; \phi_1, \varphi_{2,1}) v_{20} + i\phi_1 e^{-mt_1} x_0 \right] \\
&\cdot \exp\left[-\sum_{k=1}^{n} i\phi_k (\Delta_k \tilde{C}_1 + \Delta_k C_2 + v_{10} \Delta_k B_1 + v_{20} \Delta_k B_2) \right].
\end{aligned}$$

where $G(T)$ is the forward price with maturity T, $B_j, C_2, \varphi_{j,k}, \phi_k, j = 1, 2, k = 1, \cdots, n$ are defined in Theorem 2.1, $\tilde{C}_1$ is defined in (10) and

$$\begin{aligned}
\Delta_k \tilde{C}_1 &= \tilde{C}_1(t_k; -i, 0) - e^{-m(t_k - t_{k-1})} \tilde{C}_1(t_{k-1}; -i, 0) \\
\Delta_k C_2 &= C_2(t_k; -i, 0) - e^{-m(t_k - t_{k-1})} C_2(t_{k-1}; -i, 0) \\
\Delta_k B_j &= B_j(t_k; -i, 0) - e^{-m(t_k - t_{k-1})} B_j(t_{k-1}; -i, 0),\ j = 1, 2
\end{aligned}$$

In practice, if there are no available options to calibrate the risk-neutral parameters, it is interesting to know how to use the estimated physical parameters to infer the risk-neutral parameters, especially $\theta(t)$. In fact, we can also super-calibrate $\theta(t)$ with the physical parameters by the use of the change of measure. For simplicity, we suppose that, under the physical measure $\mathbb{P}$, the underlying asset S_t and its volatility factor V_t jointly evolve as follows. Let $S_t = \exp(X_t)$.

$$\begin{aligned}
dX_t &= [\mu - mX_t]dt + \sqrt{V_t} dZ_t^1, \\
dV_t &= [a^{\mathbb{P}} - b^{\mathbb{P}} V_t]dt + \sigma \sqrt{V_t} [\rho dZ_t^1 + \sqrt{1 - \rho^2} dZ_t^2],
\end{aligned}$$

where Z_t^1, Z_t^2 are independent standard Wiener processes under $\mathbb{P}$. By the change of measure, the joint dynamics of X_t and V_t under $\mathbb{Q}$ becomes

$$\begin{aligned} dX_t &= [\theta(t) - mX_t - \tfrac{V_t}{2}]dt + \sqrt{V_t}dW_t^1, \\ dV_t &= [a(t) - bV_t]dt + \sigma\sqrt{V_t}[\rho dW_t^1 + \sqrt{1-\rho^2}dW_t^2], \end{aligned}$$

where W_t^1, W_t^2 are independent standard Wiener processes under $\mathbb{Q}$, and

$$a(t) = a^{\mathbb{P}} - \rho\sigma(\mu - \theta(t)),\ b = b^{\mathbb{P}} + \frac{\rho\sigma}{2}. \tag{11}$$

These relations between physical and risk-neural parameters help us to establish the super-calibration of $\theta(t)$. Moreover, we assume $\theta(t)$ to be a piecewise function defined on sampling intervals: $\theta(t) = \sum_{k=1}^{n} \theta_k \mathbf{1}_{\{t\in(t_{k-1},t_k]\}}$. Using the Corollary 2.1 and noting that there is only one SV factor and no jumps, the terms related to $\theta(t)$ can be expressed as

$$\begin{aligned} &\int_0^T \theta(s)g(s,T)ds := \int_0^T \theta(s)[e^{-m(T-s)} + \rho\sigma B(T-s;-i,0)]ds \\ =\ & \ln[G(T)] - B(T;-i,0)v_0 - e^{-mT}x_0 - \check{C}(T;-i,0), \end{aligned} \tag{12}$$

where $G(T)$ is the forward price with maturity T given the initial values $X_0 = x_0, V_0 = v_0$, and $\check{C}(T;-i,0) = \int_0^T (a^{\mathbb{P}} - \rho\sigma\mu)B(T-s;-i,0)ds$. Then the recursive formula for θs is given

$$\begin{aligned} \theta_k \ =\ & \Big[\ln[G(t_k)] - B(t_k;-i,0)v_0 - e^{-mt_k}x_0 - \check{C}(t_k;-i,0) \\ & - \sum_{j=1}^{k-1}\theta_j \int_{t_{j-1}}^{t_j} g(s,t_k)ds\Big] \Big/ \left[\int_{t_{k-1}}^{t_k} g(s,t_k)ds\right], \end{aligned} \tag{13}$$

where $g(s,T) = e^{-m(T-s)} + \rho\sigma B(T-s;-i,0)$ and $\sum_{j=1}^{0}(\cdot) = 0$. Hence, we can utilize the whole futures structure to super-calibrate the drift term $\theta(t)$. We will illustrate the whole implementation with the empirical parameters in Section 4.

3. Variance swaps

Variance swaps enable investors to trade on the variance of an underlying asset. By specifying the sampling dates of a variance swap, for example $0 = t_0 < t_1 < \cdots < t_N = T$, the payoff of the contract at maturity T is defined as

$$\frac{AF}{N}\sum_{k=1}^{N} w_k \left(\ln\frac{S_{t_k}}{S_{t_{k-1}}}\right)^2 - K, \tag{14}$$

where w_k is the weight put on the return over the period $[t_{k-1}, t_k]$. The constant K is the strike price the long side of the variance swap will pay at the end of the contract. The constant AF is the annualized factor. For instance, if we consider daily sampling for the contract, that is $t_k - t_{k-1} = \frac{1}{252}$, then $AF = 252$. This section examines the analytic pricing for vanilla variance swaps, gamma swaps, corridor variance swaps and conditional variance swaps.

3.1. Vanilla variance swaps

Vanilla variance swaps are the simplest form of variance swap. Their payoffs are obtained by putting all the weights $w_k = 1$ in (14).

The fair strike price K is set in such a way that the contract has zero value at the initial time. Under the market-implied pricing measure, the no-arbitrage strike price becomes

$$K = \mathbb{E}\left[\frac{AF}{N}\sum_{k=1}^{N}\left(\ln\frac{S_{t_k}}{S_{t_{k-1}}}\right)^2\right],$$

which is often called the variance swap price/rate. Because AF and N are constants once the tenor structure for the contract is specified, the above expectation is indeed taken on each of the squared log returns one by one. By the property of characteristic function, the expectation for each term inside the above summation,

which is essentially the second moment, is calculated as:

$$\mathbb{E}\left[\left(\ln\frac{S_{t_k}}{S_{t_{k-1}}}\right)^2\right] = \frac{\partial^2}{\partial\phi^2}F_{X_{t_{k-1}},X_{t_k}}(i\phi,-i\phi)\Big|_{\phi=0}.$$

This gives the closed-form solution for the vanilla variance swap price.

When mean reversion and jumps are absent in model (1), the explicit formulas for the vanilla variance swap prices using one-factor and two-factor SV models are summarized in the following proposition. This result is used in the subsequent empirical analysis on the contribution of the second volatility factor.

Proposition 3.1. If the log-asset price $X(t)$ follows the one-factor SV model (namely Heston model, i.e. $M(\Theta;0,0)$ with $\Theta=\{\theta,0,a,b,\sigma,\rho,0\}$), then the variance swap with monitoring dates $0=t_0<t_1<\cdots<t_N=T$ has the fair price

$$VS_1(x,v,T,N;\Theta)=k_1v^2+k_2v+k_3,$$

where

$$\begin{aligned}
k_1 &= \frac{AF}{4b^2N}\sum_{k=1}^{N}e^{-2bt_{k-1}}(e^{-b(t_k-t_{k-1})}-1)^2,\\
k_2 &= \frac{AF}{N}\left(\frac{1}{b}-\frac{\rho\sigma}{b^2}+\frac{\sigma^2}{2b^3}\right)(1-e^{-bT})+\frac{AF}{N}\left(\frac{\rho\sigma}{b^2}-\frac{\sigma^2}{2b^3}\right)\sum_{k=1}^{N}be^{-bt_k}(t_k-t_{k-1})\\
&\quad -\frac{1}{b}\left(\theta-\frac{a}{2b}\right)\frac{AF}{N}\sum_{k=1}^{N}(e^{-bt_{k-1}}-e^{-bt_k})(t_k-t_{k-1})-\frac{2a+\sigma^2}{b}k_1,\\
k_3 &= \frac{AF}{N}\left(\frac{a}{b}-\frac{a\rho\sigma}{b^2}+\frac{a\sigma^2}{4b^3}\right)T+\frac{AF}{N}\left(\frac{a\rho\sigma}{b^3}-\frac{a\sigma^2}{4b^4}\right)\sum_{k=1}^{N}(1-e^{-b(t_k-t_{k-1})})\\
&\quad +\frac{AF}{N}\left(r-\frac{a}{2b}\right)^2\sum_{k=1}^{N}(t_k-t_{k-1})^2-\frac{a}{b}k_2-\frac{2a^2+a\sigma^2}{2b^2}k_1.
\end{aligned}$$

Alternatively, if $X(t)$ follows the two-factor SV model, i.e. $m = 0$ and $J_t^X, J_t^{V_1}, J_t^{V_2} \equiv 0$ in model (1), then the vanilla variance swap price is given by

$$VS_2(x, v_1, v_2, T, N) = VS_1(x, v_1, T, N; \Theta_1) + VS_1(0, v_2, T, N; \Theta_2) + I(v_1, v_2),$$

where $I(v_1, v_2) = \frac{2AF}{N}(k_4 v_1 v_2 + k_5 v_1 + k_6 v_2 + k_7)$,

$$\begin{aligned}
\Theta_1 &= \{\theta, 0, a_1, b_1, \sigma_1, \rho_1, 0\},\ \Theta_2 = \{0, 0, a_2, b_2, \sigma_2, \rho_2, 0\},\\
k_4 &= \frac{1}{4b_1 b_2}\sum_{k=1}^{N}(e^{-b_1 t_k} - e^{-b_1 t_{k-1}})(e^{-b_2 t_k} - e^{-b_2 t_{k-1}}),\ k_5 = -\frac{a_2}{b_2}k_4 - \frac{a_2}{2b_2}h(b_1),\\
k_6 &= -\frac{a_1}{b_1}k_4 + \left(\theta - \frac{a_1}{2b_1}\right)h(b_2),\ h(b) = \frac{1}{2b}\sum_{k=1}^{N}(e^{-bt_k} - e^{-bt_{k-1}})(t_k - t_{k-1}),\\
k_7 &= \frac{a_1 a_2}{b_1 b_2}k_4 + \frac{a_1 a_2}{2b_1 b_2}h(b_1) - \frac{a_2}{b_2}\left(\theta - \frac{a_1}{2b_1}\right)h(b_2) - \frac{a_2}{2b_2}\left(\theta - \frac{a_1}{2b_1}\right)\sum_{k=1}^{N}(t_k - t_{k-1})^2.
\end{aligned}$$

In addition, by taking the asymptotic limit: $\max_k(t_k - t_{k-1}) \to 0$ and $\frac{AF}{N} = \frac{1}{T}$, the two formulas respectively converge to their continuously monitoring counterparts:

$$\begin{aligned}
VS_1(x, v, T, \infty; \Theta) &= \frac{1 - e^{-bT}}{bT}v - \frac{a(1 - e^{-bT})}{b^2 T} + \frac{a}{b},\\
VS_2(x, v_1, v_2, T, \infty) &= VS_1(x, v_1, T, \infty; \Theta_1) + VS_1(0, v_2, T, \infty; \Theta_2).
\end{aligned}$$

Proof. The proof follows the previous discussion and simple calculation. □

Remark: Similar explicit formulas can be derived for models with jumps. As the corresponding expression is rather long, we put it in the Appendix A and provide the Mathematica code upon request.

Proposition 3.1 shows that the fair vanilla variance swap price is a quadratic function of initial volatility and independent of the initial asset price. In fact, the same conclusion applies to cases with jumps (see Appendix A). When the log-asset price has mean reversion, the log-asset price appears in the drift term of the

SDE, which causes the pricing formula to depend on the initial asset price. If the underlying asset is liquidly traded, the drift term can be delta-hedged away, which eliminates the mean reversion effect under a risk-neutral measure. However, if the underlying asset is not traded as a commodity, mean reversion remains in the market-implied pricing dynamic and should be taken into account in the variance swap pricing formula. In this latter situation, we expect the variance swap price to be dependent on the initial asset price.

3.2. Gamma swaps

Gamma swaps are variance swaps with weights $w_k = \frac{S_{t_k}}{S_{t_0}}$ in (14). One motivation to trade gamma swaps is to protect the swap sellers from crash risk because the weights of gamma swaps inherently dampen the downside variance. The fair strike price for a gamma swap is defined as

$$K = \mathbb{E}\left[\frac{AF}{N}\sum_{k=1}^{N}\frac{S_{t_k}}{S_{t_0}}\left(\ln\frac{S_{t_k}}{S_{t_{k-1}}}\right)^2\right].$$

The valuation requires the weight to be included in the expectation and we again use a property of the characteristic function. Specifically,

$$\begin{aligned}\mathbb{E}\left[\frac{S_{t_k}}{S_{t_0}}\left(\ln\frac{S_{t_k}}{S_{t_{k-1}}}\right)^2\right] &= \mathbb{E}\left[e^{(X_{t_k}-X_{t_0})}(X_{t_k}-X_{t_{k-1}})^2\right] \\ &= e^{-X_0}\frac{\partial^2}{\partial\phi^2}\mathbb{E}\left[e^{\phi(X_{t_k}-X_{t_{k-1}})+X_{t_{k-1}}}\right]\Big|_{\phi=1} \\ &= e^{-X_0}\frac{\partial^2}{\partial\phi^2}F_{X_{t_{k-1}},X_{t_k}}(i\phi-i,-i\phi)\Big|_{\phi=1}.\end{aligned}$$

This offers the closed-form gamma swap price through the characteristic function. When mean reversion and jumps are removed from the model (1), the explicit formulas for the gamma swap prices under the one-factor and two-factor SV models are given in the following proposition.

Proposition 3.2. If the log-asset price $X(t)$ follows the one-factor SV model, the gamma swap price with monitoring dates: $0 = t_0 < t_1 < \cdots < t_N = T$ is $GS_1(x, v, T, N; \Theta) = n_1 v^2 + n_2 v + n_3$, where

$$\begin{aligned}
n_1 &= \frac{AF}{4b^{*2}N}\sum_{k=1}^{N} e^{(\theta t_k - 2b^* t_{k-1})}(1 - e^{-b^*(t_k - t_{k-1})})^2,\ b^* = b - \rho\sigma, \\
n_2 &= \frac{AF}{N}\sum_{k=1}^{N}\left(\frac{1}{b^*}\left(\theta + \frac{a}{2b^*}\right)(t_k - t_{k-1}) + \left(\frac{1}{b^*} + \frac{\rho\sigma}{b^{*2}} + \frac{\sigma^2}{2b^{*3}}\right)\right)(e^{-b^* t_{k-1}} - e^{-b^* t_k})e^{\theta t_k} \\
&\quad -\frac{AF}{N}\left(\frac{\rho\sigma}{b^*} + \frac{\sigma^2}{2b^{*2}}\right)\sum_{k=1}^{N} e^{(\theta - b^*)t_k}(t_k - t_{k-1}) - \frac{2a + \sigma^2}{b^*}n_1,
\end{aligned}$$

$$\begin{aligned}
n_3 &= \frac{AF}{N}\left(\frac{a}{b^*} + \frac{a\rho\sigma}{b^{*2}} + \frac{a\sigma^2}{4b^{*3}}\right)\sum_{k=1}^{N} e^{\theta t_k}(t_k - t_{k-1}) - \frac{AF}{N}\left(\frac{a\rho\sigma}{b^{*3}} + \frac{a\sigma^2}{4b^{*4}}\right)\sum_{k=1}^{N} e^{\theta t_k}(1 - e^{-b^*(t_k - t_{k-1})}) \\
&\quad +\frac{AF}{N}\left(\theta + \frac{a}{2b^*}\right)^2\sum_{k=1}^{N} e^{\theta t_k}(t_k - t_{k-1})^2 - \frac{a}{b^*}n_2 - \frac{2a^2 + a\sigma^2}{2b^{*2}}n_1.
\end{aligned}$$

Alternatively, if $X(t)$ follows the two-factor stochastic volatility model, then the gamma swap price is

$$GS_2(x, v_1, v_2, T, N) = GS_1(x, v_1, T, N; \Theta_1) + GS_1(0, v_2, T, N; \Theta_2) + J(v_1, v_2),$$

where Θ_1 and Θ_2 are defined in Proposition 3.1, $J(v_1, v_2) = \frac{2AF}{N}(n_4 v_1 v_2 + n_5 v_1 + n_6 v_2 + n_7)$, $b_1^* = b_1 - \rho_1\sigma_1$, $b_2^* = b_2 - \rho_2\sigma_2$,

$$\begin{aligned}
n_4 &= \frac{1}{4b_1^* b_2^*}\sum_{k=1}^{N} e^{\theta t_k}(e^{-b_1^* t_{k-1}} - e^{-b_1^* t_k})(e^{-b_2^* t_{k-1}} - e^{-b_2^* t_k}),\ n_5 = -\frac{a_2}{b_2^*}n_4 + \frac{a_2}{2b_2^*}g(b_1^*), \\
n_6 &= -\frac{a_1}{b_1^*}n_4 + \left(\theta + \frac{a_1}{2b_1^*}\right)g(b_2^*),\ g(b) = \frac{1}{2b}\sum_{k=1}^{N} e^{\theta t_k}(e^{-bt_{k-1}} - e^{-bt_k})(t_k - t_{k-1}), \\
n_7 &= \frac{a_1 a_2}{b_1^* b_2^*}n_4 - \frac{a_1 a_2}{2b_1^* b_2^*}g(b_1^*) - \frac{a_2}{b_2^*}\left(\theta + \frac{a_1}{2b_1^*}\right)g(b_2^*) + \frac{a_2}{2b_2^*}\left(\theta + \frac{a_1}{2b_1^*}\right)\sum_{k=1}^{N} e^{\theta t_k}(t_k - t_{k-1})^2.
\end{aligned}$$

By taking $\max_k(t_k - t_{k-1}) \to 0$ and $\frac{AF}{N} = \frac{1}{T}$, the above two formulas respectively converge to their continuously monitoring counterparts:

$$\begin{aligned} GS_1(x, v, T, \infty; \Theta) &= \frac{1 - e^{(-b+\rho\sigma)T}}{(b - \rho\sigma T}v - \frac{a(1 - e^{(-b+\rho\sigma)T})}{(b - \rho\sigma)^2 T} + \frac{a}{b - \rho\sigma}, \\ GS_2(x, v_1, v_2, T, \infty) &= GS_1(x, v_1, T, \infty; \Theta_1) + GS_1(0, v_2, T, \infty; \Theta_2). \end{aligned}$$

Interestingly, the gamma swap prices remain independent of the initial log-asset price whenever there is no mean reverting effect in the asset return. Similar explicit formula for models with jumps can also be obtained. Due to long expression of it and the page limit, we omit here and provide the Mathematica code upon request.

3.3. Corridor variance swaps

The structure of corridor variance swaps is similar to that of vanilla variance swaps except that the underlying asset price must fall within a specified corridor for that period's squared log return to be included in the variance. A typical corridor variance swap sets $w_k = \mathbf{1}_{\{L < S_{t_{k-1}} \leq U\}}$ in (14).

Corridor variance swaps allow investors to take view on a particular interval of the implied volatility smile because only the realized variance within the corridor is included. A downside-variance swap sets $L = 0$ while an upside-variance swap lets $U \to \infty$. In general, the payoff of various corridor variance swaps can be spanned by downside-variance swaps and vanilla variance swaps. Hence, it is sufficient to consider the pricing of downside-variance swaps. The fair strike price for a downside-variance swap is given by

$$K = \mathbb{E}\left[\frac{AF}{N}\sum_{k=1}^{N}\left(\ln\frac{S_{t_k}}{S_{t_{k-1}}}\right)^2 \mathbf{1}_{\{S_{t_{k-1}} \leq U\}}\right].$$

The random part here is the squared log return and the indicator function. The expectation for each term in the summation is calculated as follows.

$$\mathbb{E}\left[\left(\ln\frac{S_{t_k}}{S_{t_{k-1}}}\right)^2 \mathbf{1}_{\{S_{t_{k-1}}\le U\}}\right] = \frac{\partial^2}{\partial\phi^2}\mathbb{E}\left[e^{\phi(X_{t_k}-X_{t_{k-1}})}\mathbf{1}_{\{X_{t_{k-1}}\le u\}}\right]\Big|_{\phi=0}, \qquad (15)$$

where $u = \ln U$.

When $k = 1$, the value for the above indicator function is immediately known at the initial time point. Hence,

$$\begin{aligned}
\mathbb{E}\left[\left(\ln\frac{S_{t_1}}{S_{t_0}}\right)^2 \mathbf{1}_{\{S_{t_0}\le U\}}\right] &= \frac{\partial^2}{\partial\phi^2}\mathbb{E}\left[e^{\phi(X_{t_1}-X_{t_0})}\mathbf{1}_{\{X_{t_0}\le u\}}\right]\Big|_{\phi=0} \\
&= \frac{\partial^2}{\partial\phi^2}\mathbb{E}\left[e^{\phi X_{t_1}}\right]e^{-\phi X_{t_0}}\mathbf{1}_{\{X_{t_0}\le u\}}\Big|_{\phi=0} \\
&= \frac{\partial^2}{\partial\phi^2}F_{X_{t_0},X_{t_1}}(i\phi,-i\phi)\mathbf{1}_{\{X_{t_0}\le u\}}\Big|_{\phi=0}.
\end{aligned}$$

When $k \ge 2$, the expectation in (15) needs the Fourier transformation technique to deal with the indicator function. We first transform the indicator function $\mathbf{1}_{\{S_{t_{k-1}}\le U\}}$ into $\mathbf{1}_{\{X_{t_{k-1}}\le u\}}$ and consider the generalized Fourier transform on the indicator function $\mathbf{1}_{\{X_{t_{k-1}}\le u\}}$, which is a function of u.

$$\int_{-\infty}^{\infty}\mathbf{1}_{\{X_{t_{k-1}}\le u\}}e^{-iuw}du = \int_{X_{t_{k-1}}}^{\infty}e^{-iuw}du = \frac{e^{-iX_{t_{k-1}}w}}{iw}.$$

The complex variable w in the Fourier transform is written as $w = w_r + iw_i$. Then, the Fourier transform exists for $w_i \in (-\infty, 0)$. By taking the inverse Fourier transform, the quantity $\mathbf{1}_{\{X_{t_{k-1}}\le u\}}$ can be expressed in the Fourier integral form:

$$\mathbf{1}_{\{X_{t_{k-1}}\le u\}} = \frac{1}{2\pi}\int_{-\infty}^{\infty}e^{iuw}\frac{e^{-iX_{t_{k-1}}w}}{iw}dw_r.$$

By replacing $\mathbf{1}_{\{X_{t_{k-1}}\le u\}}$ in (15) with its Fourier integral expression, the following

result holds.

$$
\begin{aligned}
& \mathbb{E}\left[\left(\ln\frac{S_{t_k}}{S_{t_{k-1}}}\right)^2 \mathbf{1}_{\{S_{t_{k-1}}\le U\}}\right] \\
= \; & \mathbb{E}\left[\frac{\partial^2}{\partial\phi^2} e^{\phi(X_{t_k}-X_{t_{k-1}})}\frac{1}{2\pi}\int_{-\infty}^{\infty} e^{iuw}\frac{e^{-iX_{t_{k-1}}w}}{iw}dw_r\right]\Bigg|_{\phi=0} \\
= \; & \frac{e^{-uw_i}}{\pi}\int_0^{\infty} Re\left(\frac{e^{iuw_r}}{iw_r-w_i}\frac{\partial^2}{\partial\phi^2}\mathbb{E}\left[e^{\phi X_{t_k}-(\phi+iw)X_{t_{k-1}}}\right]\Bigg|_{\phi=0}\right)dw_r \\
= \; & \frac{e^{-uw_i}}{\pi}\int_0^{\infty} Re\left(\frac{e^{iuw_r}}{iw_r-w_i}\frac{\partial^2}{\partial\phi^2}F_{X_{t_{k-1}},X_{t_k}}(i\phi-w,-i\phi)\Big|_{\phi=0}\right)dw_r.
\end{aligned}
$$

This integration can be efficiently made by utilizing the fast Fourier transform (FFT) technique, a numerical technique introduced in Carr and Madan, 1999. This procedure is repeated for $k = 2, \cdots, N$. We compute the fair corridor variance swap price by summing up all the individual terms obtained in the early computation and then multiplying the sum with the constant $\frac{AF}{N}$.

3.4. Conditional variance swaps

A conditional variance swap is similar to a corridor variance swap, except that the summation of the squared log return is divided by D, the number of asset prices that fall within the corridor, rather than N. The final payoff is then adjusted by the factor $\frac{D}{N}$. Therefore, the conditional variance swap payoff is

$$
\begin{aligned}
& \frac{D}{N}\left[\frac{AF}{D}\sum_{k=1}^{N}\left(\ln\frac{S_{t_k}}{S_{t_{k-1}}}\right)^2 \mathbf{1}_{\{S_{t_{k-1}}\le U\}} - K\right] \\
= \; & \left[\frac{AF}{N}\sum_{k=1}^{N}\left(\ln\frac{S_{t_k}}{S_{t_{k-1}}}\right)^2 \mathbf{1}_{\{S_{t_{k-1}}\le U\}} - K'\right] + \left(K' - K\frac{D}{N}\right),
\end{aligned}
$$

where $D = \sum_{k=1}^{N} \mathbf{1}_{\{S_{t_{k-1}}\le U\}}$ and K' is the fair corridor variance swap price.

Conditional variance swaps offer an alternative to trade variance within a corridor other than the corridor swap. A possible advantage of using conditional

variance swaps is that their strikes are adjusted by $\frac{D}{N}$, hence the profit is immune from the time the underlying asset is within the corridor. The payoff structure however shows that the conditional variance swap can be fully replicated by a corridor variance swap and a range accrual note (RAN). Hence, it remains for us to compute the RAN, $\mathbb{E}(D)$, with the proposed model. Then, $K = K' \frac{N}{\mathbb{E}(D)}$.

The calculation $\mathbb{E}(D)$ can be made by summing up $\mathbb{E}(\mathbf{1}_{\{S_{t_{k-1}} \leq U\}})$ for $k = 1, \ldots, n$. For $k = 1$, $\mathbb{E}(\mathbf{1}_{\{S_{t_0} \leq U\}}) = \mathbf{1}_{\{S_{t_0} \leq U\}}$. For $k \geq 2$, we express $\mathbf{1}_{\{S_{t_{k-1}} \leq U\}} = \mathbf{1}_{\{X_{t_{k-1}} \leq u\}}$ in a Fourier integral form. Hence,

$$\begin{aligned} \mathbb{E}(\mathbf{1}_{\{S_{t_{k-1}} \leq U\}}) &= \mathbb{E}\left(\frac{1}{2\pi} \int_{-\infty}^{\infty} e^{iuw} \frac{e^{-iX_{t_{k-1}} w}}{iw} dw_r \right) \\ &= \frac{e^{-uw_i}}{\pi} \int_0^{\infty} Re\left(\frac{e^{iuw_r}}{iw_r - w_i} F_{X_{t_{k-1}}, X_{t_k}}(-w, 0) \right) dw_r. \end{aligned}$$

The conditional variance swap price is then obtained by combining the corresponding corridor variance swap price and value of $\mathbb{E}(D)$.

4. Numerical and empirical studies

This section investigates the accuracy and efficiency of the pricing solution and empirically examines the contribution of the second volatility factor. The accuracy of our analytical pricing methodology is benchmarked against a simulation. We examine the effect of monitoring frequency on the fair strike. We also examine the effect of the second volatility factor on variance swap prices when the model is calibrated to the volatility surface implied by the market prices of options. The empirical results favor the two SV model. Due to the page limit, the price sensitivities of the variance swaps to mean reversion and jumps are included in the online supplement material. As such, we focus on the contribution of the second volatility factor to the value of variance swaps.

4.1. Effect of monitoring frequency

The numerical comparison is based on the four aforementioned types of variance swaps under different sampling frequencies. The MC simulation adapts the Euler-Maruyama discretization scheme, where the dynamics for the log asset price and the two stochastic factors are discretized as follows.

$$\begin{aligned} V_{jt_k} &= \max\left(V_{jt_{k-1}} + (a_j - b_j V_{jt_{k-1}})\delta t + \sigma_j \sqrt{V_{jt_{k-1}}\delta t} Z_j + J^{V_j} Y_j, 0\right),\ j = 1, 2, \\ X_{t_k} &= X_{t_{k-1}} + \left(\theta - m X_{t_{k-1}} - \frac{V_{1t_{k-1}} + V_{2t_{k-1}}}{2}\right)\delta t + J^X Y_1 \\ &+ \sqrt{V_{1t_{k-1}}\delta t}\left(\rho_1 Z_1 + \sqrt{1-\rho_1^2} Z_3\right) + \sqrt{V_{2_{t_{k-1}}}\delta t}\left(\rho_2 Z_2 + \sqrt{1-\rho_2^2} Z_4\right), \end{aligned}$$

where δt is the simulation time step; J^{V_1} and J^{V_2} are independent exponential random variables with means η_1 and η_2, respectively; $J^X | J^{V_1} \sim \mathcal{N}(\nu + \rho_J J^{V_1}, \delta^2)$; and Z_1, Z_2, Z_3 and Z_4 are independent standard normal random variables. The independent Bernoulli random variables Y_1 and Y_2 with parameters $\lambda_1 \delta t$ and $\lambda_2 \delta t$ approximate Poisson processes with arrival rates of λ_1 and λ_2, respectively. To match the monitoring frequency specified in the variance swap contracts, the time step is set such that the sets of monitoring dates are subsets of the set of dates of simulated prices. Specifically, the simulation divides the one year maturity of the variance swaps into $252 \times 26 = 3276$ subintervals for daily monitoring contracts when there are 252 trading days a year. More precisely, the simulation uses $\delta t = \frac{1}{3276}$ and 1 million sample paths. Table 1 summarizes the parameter values used in the numerical experiment. These parameter values are obtained by rescaling the empirical two-factor SV parameters in Table 3 to retain the first two moments. For simple illustration, we use a constant θ, a_1 and a_2.

Table 2 compares the analytic and simulated fair strike prices for the variance swaps under different sampling frequencies. The analytic results in Zheng and

Kwok (2012) are included for comparison. The simulation standard deviations are in parentheses. The fair strike values and standard deviations are measured in variance points, which equal the realized variance multiplied by 100^2. The same expression is used for the remaining parts of the paper. The relative errors of the analytic solutions against the simulated solutions in Table 2 show that they closely match for all cases, verifying the accuracy of the analytic solution. However, the analytical pricing procedure is much more efficient. Specifically, the execution time for the analytical solution of vanilla and gamma swaps are 0.02% to 0.3% of that to simulate one price, depending on the monitoring frequency. The execution time of corridor swap is higher but still much faster than the simulation.

Table 1: Model parameter values

S_0	1	V_{10}	0.0076	V_{20}	0.1076
θ	0.0787	a_1	0.0277	a_2	0.1277
ρ_1	-0.82	b_1	3.56	b_2	3.66
ρ_2	-0.72	σ_1	0.14	σ_2	0.24
m	3.46	λ_1	0.47	λ_2	0.57
ρ_J	0.2	η_1	0.3	η_2	0.4
ν	-0.086	δ	0.0001		

Table 2: Comparison of fair strike prices for various types of variance swaps

		Monitoring frequency (N)						
		1	2	4	12	26	52	252
Vanilla variance swaps	Analytic solution	216.3	539.0	859.1	1179.6	1285.7	1334.2	1373.9
	Simulated solution	216.1 (0.5)	539.3 (1.1)	860.3 (1.3)	1181.1 (1.3)	1288.0 (1.2)	1335.9 (1.2)	1375.4 (1.2)
	Relative error	0.11%	-0.06%	-0.14%	-0.12%	-0.18%	-0.12%	-0.10%
Gamma swaps	Analytic solution in [12]	N/A	N/A	171.0	170.0	169.9	169.9	169.8
	Analytic solution	210.4	530.7	850.1	1170.2	1275.5	1323.3	1362.4
	Simulated solution	209.9 (0.5)	531.0 (1.1)	851.6 (1.3)	1171.8 (1.3)	1277.8 (1.2)	1324.9 (1.2)	1363.8 (1.2)
	Relative error	0.26%	-0.07%	-0.18%	-0.14%	-0.18%	-0.13%	-0.10%
Corridor variance swaps ($U = S_0$)	Analytic solution in [12]	N/A	N/A	110.5	101.0	99.7	99.2	99.0
	Analytic solution	216.3	370.6	518.2	663.2	710.4	731.5	748.7
	Simulated solution	216.1 (0.5)	371.8 (1.1)	519.6 (1.4)	664.2 (1.6)	713.1 (1.6)	734.4 (1.6)	751.9 (1.6)
	Relative error	0.11%	-0.32%	-0.28%	-0.15%	-0.39%	-0.39%	-0.43%
Conditional variance swaps ($U = S_0$)	Analytic solution in [12]	N/A	N/A	213.7	244.6	258.3	265.2	271.1
	Analytic solution	216.3	506.8	865.6	1298.0	1457.3	1532.4	1595.2
	Simulated solution	216.1 (0.4)	509.4 (0.8)	871.5 (1.0)	1307.7 (1.1)	1472.2 (1.9)	1548.3 (1.6)	1612.7 (1.9)
	Relative error	0.11%	-0.50%	-0.68%	-0.74%	-1.01%	-1.03%	-1.09%

4.2. Effect of the second volatility factor

To empirically show the effect of the second volatility factor on variance swaps, the computation is based on parameters calibrated to real option data. Christoffersen et al. (2009) calibrated the one-factor and two-factor SV models to S&P 500 index option prices. Their calibration results are reported in Table 3, where we supplement some of the missing values with our own efforts. We remark here that the Feller conditions for SV factors should be imposed within the calibration. Based on this set of option prices, Christoffersen et al. (2009) report that the two-factor model offers better in-sample and out-sample fits than the one-factor model.

Table 3: Calibrated parameters to S&P 500 index option data reported by Christoffersen et al. (2009)

One-factor SV parameters						Two-factor SV parameters					
S_0	358.76	V_{10}	0.07	V_{20}	0	S_0	358.76	V_{10}	0.02	V_{20}	0.05
θ	0.0764	a_1	0.1160	a_2	0	θ	0.0764	a_1	0.0054	a_2	0.2320
ρ_1	-0.6717	b_1	1.9561	b_2	0	ρ_1	-0.7695	b_1	0.2370	b_2	8.4983
ρ_2	0	σ_1	0.8516	σ_2	0	ρ_2	-0.8417	σ_1	1.0531	σ_2	0.6827

When these calibrated parameters are fed into the pricing formulas, range differences in variance swap prices can be observed between the two SV models. The prices for the variance swaps under the different models are shown in Table 5. The relative price difference is measured as the price from the two-factor model less the price from the one-factor model and then divided by the price of the one-factor model. It can be seen from Table 5 that the variance swap prices are very differ-

ent under the different models. Typically, the one-factor SV model overestimates various types of variance swap prices by more than 17% for all cases compared to the two-factor SV model. As the two-factor SV model better captures the implied volatility surface, derivative traders who use implied volatility information in their daily work may consider the variance swap prices from the one-factor SV model as too expensive. The second volatility factor offers a reason to lower the price to better integrate the information on implied volatility into the valuation. We also observe the relative error increases with the monitoring frequency. This is because a two factor volatility model explains the volatility surface significantly better than a single factor volatility model. This makes the price under the two models evolves very differently. When the monitoring frequency increases, more sample points are included and the difference is more obvious.

We further compare the variance swap price differences between our model and the model of Zheng and Kwok (2012). We continue to use the parameters in Table 3, except for the jump part we follow the values in Table 1. Results are given in Table 6. We see that the price differences between the two models are huge but the price patterns across monitoring frequency are similar.

4.3. Super-calibration

We are able to calibrate our model based on market information. The functional value of $\theta(t)$ in our model could be super-calibrated to futures, while other parameter values could be calibrated based on option prices. The characteristic function obtained would be in terms of the future price curve, and it could be used to price variance swaps. Even that there are only estimated physical parameters, we can also super-calibrate $\theta(t)$ in terms of them by the discussion at the end of Section 2. Based on this idea, we illustrate how to calibrate a mean reversion one-

factor SV model for wheat price. We first take the values estimated by Lahiani et al. (2013) using a VAR-GARCH model. Some missing values are supplemented by us to the best of our knowledge. The parameters values are reported in Table 4. We can adopt the estimated parameter values as our model is a continuous case of their model. We then calibrate the θs using the recursive formula (13) by the future price curve observed on 19th November 2013. The futures price with maturity $\frac{1}{12}$, $\frac{1}{3}$, $\frac{1}{2}$, $\frac{2}{3}$, $\frac{5}{6}$ and $\frac{13}{12}$ are 646.6, 656.2, 659.4, 657, 665 and 676.5 respectively. The resulting $\{\theta_k\}_{k=1}^6$ ($\theta(t) = \sum_{k=1}^6 \theta_k \mathbf{1}_{\{t\in(t_{k-1},t_k]\}}$) are 2.2976, 5.3308, 5.3231, 5.2848, 5.3955, 5.4199. We can then obtain the risk-neural parameters a and b by (11). The pricing follows previous sections. The fair strikes for vanilla variance swaps and gamma swaps with the monitoring dates set as the futures maturity dates are 3800.5 and 3112.0 (in variance points) respectively.

Table 4: Physical parameter values for calibration

S_0	834.36	V_0	0.1628	$a^{\mathbb{P}}$	0.000065	$b^{\mathbb{P}}$	0.0677
μ	0.000217	m	0.8115	σ	0.0674	ρ	1

5. Conclusion

In this paper, we derive the analytical fair strike price for various types of variance swaps when the underlying asset exhibits mean reversion, multivariate stochastic volatility and jumps. The pricing method relies on using the bivariate characteristic function for the log asset price at two different time points. When pricing the corridor variance swap and the conditional variance swap, the analytical solution is expressed in terms of Fourier integrals. We confirm the accuracy

and efficiency of the analytical results by benchmarking the analytical pricing formulas against Monte Carlo simulation. We further examine the effect of the second volatility factor on variance swap prices. The results show that the effect of the second volatility factor is very significant, which supports using the proposed model for variance swap pricing. Moreover, the proposed model can be calibrated to fit the volatility surface implied by the market prices of options. We believe that the analytical results obtained in this paper will be useful for practitioners who are eager to estimate variance swap prices consistent with the observed implied volatility surface. Apart from variance swaps, our model can be used to price a wide scope of derivatives. This can be achieved by using the multivariate characteristic function and Fourier transform technique. The performance of such application requires further investigation.

References

[1] P. Carr and D. Madan, Towards a theory of volatility trading, in R. Jarrow (ed.), Volatility (London: Risk Books, 1998) 417-427.

[2] P. Carr and D. Madan, Option valuation using the fast Fourier transform, Journal of Computational Finance 2 (1999) 61-73.

[3] P. Christoffersen, S. Heston and K. Jacobs, The shape and term structure of the index option smirk : Why multifactor stochastic volatility models work so well, Management Science 55 (2009) 1914-1932.

[4] K. Demeterfi, E. Derman, M. Kamal, J. Zou, A guide to volatility and variance swaps, Journal of Derivatives, summer (1999) 9-32.

[5] D. Duffie, J. Pan and K. Singleton, Transform analysis and asset pricing for affine jump-diffusions, Econometrica 68 (2000) 1343-1376.

[6] G. Fusai, M. Marena and A. Roncoroni, Analytical pricing of discretely monitored Asian-style options: Theory and application to commodity markets, Journal of Banking & Finance 32 (2008) 2033-2045.

[7] J. Jacod and V. Todorov, Do price and volatility jump together?, The Annals of Applied Probability 20 (2010) 1425-1469.

[8] A. Lahiani, D.K. Nguyen and T. Vo, Understanding return and volatility spillovers among major agricultural commodities, The Journal of Applied Business Research 29 (2013) 1781-1790.

[9] G. Li and C. Zhang, On the number of state variables in options pricing, Management Science 56 (2010) 2058-2075.

[10] H.Y. Wong and Y.W. Lo, Option pricing with mean reversion and stochastic volatility, European Journal of Operational Research 197 (2009) 179-187.

[11] H.Y. Wong and J. Zhao, Currency option pricing: Mean reversion and multiscale stochastic volatility, The Journal of Futures Markets 30 (2010) 938-956.

[12] W.D. Zheng and Y.K. Kwok, Closed form pricing formulas for discretely sampled generalized variance swaps, Mathematical Finance (2012) doi: 10.1111/mafi.12016.

[13] W.D. Zheng and Y.K. Kwok, Saddlepoint approximation methods for pric-

ing derivatives on discrete realized variance, Applied Mathematical Finance (2013a), forthcoming.

[14] W.D. Zheng and Y.K. Kwok, Fourier transform algorithms for pricing and hedging discretely sampled exotic variance products and volatility derivatives under additive processes, Journal of Computational Finance (2013b), forthcoming.

[15] S.-P. Zhu and G.-H. Lian, A closed-form exact solution for pricing variance swaps with stochastic volatility, Mathematical Finance 21 (2011) 233-256.

Table 5: Comparison of fair strike prices for various types of variance swaps under different models

		Monitoring frequency (N)						
		1	2	4	12	26	52	252
Vanilla variance swaps	One-factor	777.9	725.9	688.8	657.8	648.4	644.2	640.9
	Two-factor	638.9	581.3	547.2	519.5	510.8	506.8	503.5
	Relative error	-17.87 %	-19.92 %	-20.56 %	-21.02 %	-21.23 %	-21.33 %	-21.43 %
Gamma swaps	One-factor	626.4	582.4	569.8	566.4	566.4	566.5	566.7
	Two-factor	482.9	448.2	435.2	430.7	430.6	430.8	431.0
	Relative error	-22.91 %	-23.05 %	-23.62 %	-23.97 %	-23.98 %	-23.96 %	-23.93 %
Corridor variance swaps ($U = S_0$)	One-factor	777.9	573.0	495.6	453.5	442.8	437.3	431.9
	Two-factor	638.8	464.4	390.4	336.2	325.6	320.9	317.8
	Relative error	-17.87 %	-18.95 %	-21.23 %	-25.86 %	-26.47 %	-26.62 %	-26.41 %
Conditional variance swaps ($U = S_0$)	One-factor	777.9	861.6	984.7	1135.0	1189.7	1213.0	1229.4
	Two-factor	638.8	694.1	768.5	830.4	861.5	875.8	889.7
	Relative error	-17.87 %	-19.44 %	-21.96 %	-26.84 %	-27.59 %	-27.79 %	-27.63 %

Table 6: Comparison of fair strike prices for various types of variance swaps under different models with jump

		Monitoring frequency (N)						
		1	2	4	12	26	52	252
Vanilla variance swaps	One-factor	1251.8	1188.6	1137.8	1092.0	1077.7	1071.2	1065.9
	Two-factor	1519.0	1394.8	1300.1	1221.2	1197.1	1186.3	1177.5
	Relative error	21.35%	17.35%	14.27%	11.82%	11.08%	10.75%	10.47%
Gamma swaps	One-factor	1043.6	989.9	973.5	968.6	968.4	968.5	968.6
	Two-factor	1056.6	1014.9	1002.8	1001.7	1002.9	1003.8	1004.6
	Relative error	1.25%	2.52%	3.02%	3.41%	3.56%	3.64%	3.71%
Corridor variance swaps ($U = S_0$)	One-factor	1251.8	881.3	758.5	705.5	694.8	690.2	683.1
	Two-factor	1519.0	1018.3	892.3	776.4	762.2	756.3	751.2
	Relative error	21.35%	15.55%	17.64%	10.04%	9.71%	9.58%	9.98%
Conditional variance swaps ($U = S_0$)	One-factor	1251.8	1359.2	1484.2	1637.0	1716.7	1753.3	1774.8
	Two-factor	1519.0	1534.2	1679.8	1827.4	1865.3	1902.0	1931.5
	Relative error	21.35%	12.88%	13.18%	11.63%	8.66%	8.48%	8.83%

Appendix A. Vanilla variance swap prices under the models with jumps

If the log-asset price $X(t)$ follows the one-factor SV model with jumps (i.e. $M(\Theta; J^X, J^V)$ with $\Theta = \{\theta, 0, a, b, \sigma, \rho, \lambda\}$, $J^V \sim \exp(\eta)$ and $J^V \sim N(\nu + \rho_J J^V, \delta^2)$), then the vanilla variance swap with monitoring dates $0 = t_0 < t_1 < \cdots < t_N = T$ has the fair price

$$VS_1'(x, v, T, N; M(\Theta; J^X, J^V)) = k_1 v^2 + (k_2 + k_2^J)v + k_3 + k_3^J,$$

where k_1, k_2 and k_3 are defined in Proposition 3.1, and

$$\begin{aligned}
k_2^J &= -\frac{A}{2b^3 N}\sum_{k=1}^{N}\left[\lambda\eta(e^{-bt_{k-1}} - e^{-bt_k})^2\right. \\
&\quad \left.+(2b^2\lambda\nu + 2b^2\lambda\eta\rho_J - b\lambda\eta)(e^{-bt_{k-1}} - e^{-bt_k})(t_k - t_{k-1})\right], \\
k_3^J &= \frac{A}{8b^4 N}\sum_{k=1}^{N}\Big\{e^{-2bt_k}(e^{b(t_k - t_{k-1})} - 1)\lambda\eta\left[e^{b(t_k - t_{k-1})}(4a + 2\eta\lambda + \sigma^2 - 2b\eta)\right. \\
&\quad +e^{b(t_k + t_{k-1})}(8b^2(\nu + 2\eta\rho_J) - 2\sigma^2 - 4b\eta + 8b\rho\sigma) + e^{bt_k}(8\rho\sigma - 8b^2 - 4\sigma^2) \\
&\quad \left.-2\eta\lambda - 2b\eta - \sigma^2 + 2b\eta\right] \\
&\quad +(t_k - t_{k-1})2b\lambda\left[e^{-bt_{k-1}}[4b(a\nu + \eta^2\lambda\rho_J + \eta(\theta + \lambda\nu + a\rho_J)) - 2\lambda\eta^2]\right. \\
&\quad +e^{-bt_k}\left[-4b(a\nu + \eta^2\lambda\rho_J + \eta(\theta + \lambda\nu + a\rho_J + \rho\sigma)) - 2\eta(2a - \lambda\eta - \sigma^2)\right] \\
&\quad \left.+4\eta b^2(1 - \nu - 2\eta\rho_J) + 4b^3(\delta^2 + \nu^2 + 2\eta\nu\rho_J + 2\eta^2\rho_J^2) + \eta\sigma^2 + 2b\eta(\eta - 2\rho\sigma)\right] \\
&\quad -(t_k - t_{k-1})^2 2b^2\lambda(2b\nu + \eta(2b\rho_J - 1))(2a + \eta\lambda - 2b(2\theta + \lambda\nu + \eta\lambda\rho_J))\Big\}.
\end{aligned}$$

Alternatively, if we consider two-factor stochastic volatility model with jumps (i.e. model (1) with $m = 0$), then the vanilla variance swap price is given by

$$\begin{aligned}
VS_2^J(x, v_1, v_2, T, N) &= I^J(v_1, v_2) + VS_1^J(x, v_1, T, N; M(\Theta_1; J^X, J^{V_1})) \\
&\quad +VS_1^J(x, v_2, T, N; M(\Theta_2; 0, J^{V_2})),
\end{aligned}$$

where $I^J(v_1, v_2) = I(v_1, v_2) + \frac{2A}{N}(k_5^J v_1 + k_6^J v_2 + k_7^J)$, $I(v_1, v_2)$ is defined in Proposition 3.1, and

$$
\begin{aligned}
k_5^J &= -\sum_{k=1}^{N}\left[\frac{(e^{-b_1 t_k} - e^{-b_1 t_{k-1}})(e^{-b_2 t_k} - e^{-b_2 t_{k-1}})\eta_2\lambda_2}{4b_1 b_2^2}\right. \\
&\quad \left. + \frac{(e^{-b_1 t_k} - e^{-b_1 t_{k-1}})\eta_2\lambda_2(t_k - t_{k-1})}{4b_1 b_2}\right], \\
k_6^J &= -\sum_{k=1}^{N}\left[\frac{(e^{-b_1 t_k} - e^{-b_1 t_{k-1}})(e^{-b_2 t_k} - e^{-b_2 t_{k-1}})\eta_1\lambda_1}{4b_1^2 b_2}\right. \\
&\quad \left. + \frac{(e^{-b_2 t_k} - e^{-b_2 t_{k-1}})(\eta_1 - 2b_1(\nu + \rho_J\eta_1))\lambda_1(t_k - t_{k-1})}{4b_1 b_2}\right], \\
k_7^J &= \sum_{k=1}^{N}\left\{\frac{(e^{-b_1 t_k} - e^{-b_1 t_{k-1}})(e^{-b_2 t_k} - e^{-b_2 t_{k-1}})[a_2\eta_1\lambda_1 + (a_1 + \eta_1\lambda_1)\eta_2\lambda_2]}{4b_1^2 b_2^2}\right. \\
&\quad + \left[(a_2 b_1\lambda_1\eta_1 + a_1 b_1\lambda_2\eta_2 + b_1\eta_1\eta_2\lambda_1\lambda_2 - 2b_1^2\eta_2\lambda_2\theta - 2b_1^2\lambda_1(\nu + \rho_J\eta_1)(a_2\lambda_1 + \eta_2\lambda_2))\right. \\
&\quad \left.(e^{-b_2 t_k} - e^{-b_2 t_{k-1}}) + (a_2 b_2\lambda_1\eta_1 + a_1 b_2\eta_2\lambda_2 + b_2\eta_1\eta_2\lambda_1\lambda_2)(e^{-b_1 t_k} - e^{-b_1 t_{k-1}})\right]\frac{t_k - t_{k-1}}{4b_1^2 b_2^2} \\
&\quad \left. + \frac{a_2\lambda_1(\eta_1 - 2b_1(\nu + \rho_J\eta_1)) + \eta_2\lambda_2(a_1 + \eta_1\lambda_1 - 2b_1(\theta + \nu\lambda_1 + \rho_J\eta_1\lambda_1))}{4b_1 b_2}(t_k - t_{k-1})^2\right\}.
\end{aligned}
$$

Appendix B. Parameter sensitivity

This appendix further investigates the effects of the mean reverting speed, m, and the jump arrival rate, λ, on fair strike prices using the two-factor SV parameters in Table 3, and observe how the fair strike prices for vanilla and gamma swaps change with the mean reversion speed and jump arrival rate. When studying the effect of λ, we also put $\eta_1 = \eta_2 = 0.05, \nu = -0.086, \rho_J = -0.38, \delta = 0.0001$. The results are presented in Figure B.1 to Figure B.2.

The fair strike prices for both vanilla variance swaps and gamma swaps can be seen to increase with m. This is somewhat counterintuitive, as we know m is the mean reversion speed for the log asset price. The larger the m, the faster the asset will return to its long term mean level, which ought to lower the volatility of the asset price. Although this is conceptually correct, the numerical example, is based on the situation where the initial log asset price x_0 is much higher than the long term mean level $\frac{\theta}{m}$. If we increase m, two effects contribute to the rise in asset volatility. First, the speed in which the asset price drops to its long term mean level is increased. Second, the long term mean level is lowered, causing an increase in the drop magnitude. This explains why a higher m will result in a higher fair strike in this case. Another result worth noting is that the increase in price for the gamma swap is much lower than that for the vanilla variance swap. This difference is due to the payoff structure of gamma swaps, we use the asset value ratio $\frac{S_{t_k}}{S_{t_0}}$ as the weight. When the asset value drops quickly, the increase in variance is counterbalanced by the decrease in weight. This effectively protects the gamma swap seller from crash risk.

In Figure B.2, the fair strike for both variance swaps increases with λ. In this case, higher jump intensity implies a higher expected number of jumps, which in-

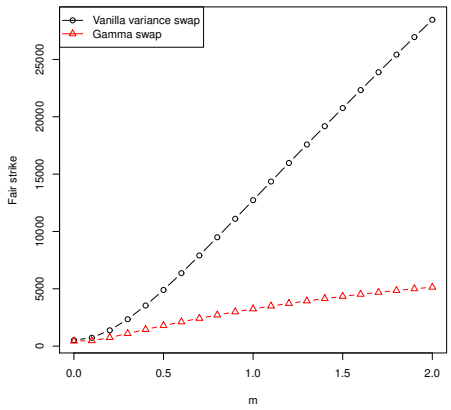

Figure B.1: Change of fair price across m

creases the asset price volatility. Interestingly, the contribution of λ_1 in increasing the fair strike price is greater than that of λ_2. This is not surprising as λ_1 is the intensity of simultaneous jumps in both log asset price and the first SV factor, while λ_2 only controls the number of jumps in the second volatility factor. The vanilla variance swap is also more sensitive to the change in λ_1 compared to the gamma swap, but the sensitivity to λ_2 is the same for both types of variance swaps. Here, the mean for the jump size in the log asset process is $\nu + \rho_J \eta_1 = -0.105$, which is a negative value for the parameter values used. If we increase λ_1, more jumps are expected in the log asset process, causing a negative jump size on average. In this case, the payoff structure for the gamma swap provides an embedded damping effect for downside variance and hence the change in fair strike for the gamma swap is smaller than that for the vanilla variance swap. When increasing λ_2, there is no directional effect on the log asset price and the price change is the same for both the vanilla variance swap and the gamma swap.

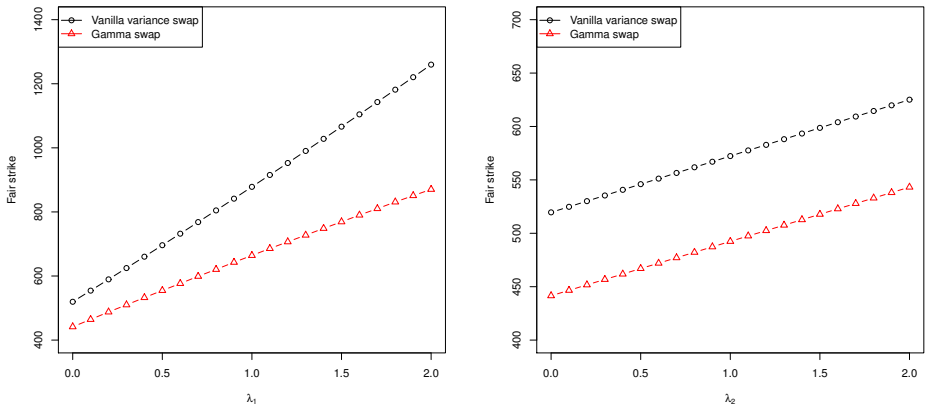

Figure B.2: Change of fair price across λ